Supporting Online Material for

Structural Basis of Immune Evasion at the Site of CD4 Attachment on HIV-1 gp120

Lei Chen, Young Do Kwon, Tongqing Zhou, Xueling Wu, Sijy O'Dell, Lisa Cavacini, Ann J. Hessell, Marie Pancera, Min Tang, Ling Xu, Zhi-yong Yang, Mei-Yun Zhang, James Arthos, Dennis R. Burton, Dimiter S. Dimitrov, Gary J. Nabel, Marshall R. Posner, Joseph Sodroski, Richard Wyatt, John R. Mascola, Peter D. Kwong*

*To whom correspondence should be addressed. E-mail: pdkwong@nih.gov

Published 20 November 2009, *Science* **326**, 1123 (2009)
DOI: 10.1126/science.1175868

This PDF file includes:

Supporting Online Material

MATERIALS AND METHODS

Neutralization Assay

Neutralization assays were performed using single round infection of HIV-1 Env-pseudoviruses to TZM-bl cells as described previously (*S1, 2*). The viruses used included well characterized clade B and clade C reference isolates (*S1, 3*). To determine the antibody concentration that results in a 50% or 80% reduction in viral entry, serial dilution assays were performed and the neutralization dose-response curves were fit by non-linear regression using a 4-parameter hill slope equation.

The adsorption of HIV-1 Env specific antibodies from serum IgG was performed on tosylactivated magnetic beads coupled to the YU2 strain of gp120 or to the CD4-binding site (CD4BS) knock out mutant gp120 D368R, as previously described (*S1, 2*). Prior to adsorption, serum IgG was purified using a protein G resin (Thermo Scientific, Inc) according to the manufacturer's instructions. See Tables S1 and S8 for detailed neutralization profiles of CD4, patient serum IgG and gp120-reactive antibodies.

Production of antigen-binding fragments (Fab) from IgG

CD4BS antibodies F105, F91, 15e, and V3-loop binding antibodies G3-299 and G3-42 IgGs were expressed as previously described (*S4*). IgGs were purified with protein A affinity column and then reduced with 100 mM DTT for 1hr at 37^{o}C. After dialyzing out the DTT, the IgG solution was alkylated by dialyzing against 2 mM Iodoactamide for 48 hrs at 4^{o}C. Activated Papain beads (for G3-299 and G3-42) or Lys-C (for other IgGs) were used to generate antibody-binding fragment (Fab) according to vendor's standard protocol (Pierce

and Roche). The Fab was further purified by protein A affinity column and size-exclusion chromatography (Superdex S200).

The b13 IgG expression plasmids for heavy and light chains were constructed by fusing genes of the b13 variable regions with constant regions from the IgG b12 expression plasmids and codon-optimized with human preferences. b13 IgG was expressed by co-transfecting 293F cells with both heavy and light chain plasmids and was purified through protein G affinity column. The antibody was then cleaved with Lys-C protease (Roche) to produce Fab. Affinity (Protein G), size-exclusion (Superdex S200) and ion-exchange (Mono-S) chromatography were used sequentially to separate the Fab from other fragments.

Deglycosylation, complex formation and crystallization of the gp120:F105 complex

YU2 and JR-FL gp120 were produced by a Drosophila Schneider 2 line under an inducible metallothionein promoter and purified by affinity chromatography as described previously (*S5*). Glycans were removed by digestion with endoglycosidase H and D to leave only proximal N-acetylglucosamine and 1,6 fucose residues.

Preparations of gp120 complexes followed procedures that were essentially the same as previously described (*S6*). Briefly, F105 Fab was added to deglycosylated gp120 and the gp120:F105 complex was passed through a concanavalin A column to remove uncleaved N-linked glycans. The complex was then purified by size exclusion chromatography (Hiload 26/60 Superdex S200 prep grade, GE Health). To make a ternary complex, Fab of the V3 loop binding antibodies was added and further purified with a Superdex S200 column, and concentrated to 5-10 mg/ml in 0.35 M NaCl, 2.5 mM Tris pH 7.0, 0.02% NaN_3 (See Table S1 for a list of gp120-CD4BS Ab complexes).

Commercially available screens, Hampton Crystal Screen (Hampton Research), Precipitant Synergy Screen (Emerald BioSystems), and Wizard Screen (Emerald BioSystems), were used. Vapor-diffusion seating drop crystallization trials of the gp120 complexes were set up robotically (Honeybee) (0.2 µl protein + 0.2 µl precipitant). Droplets were allowed to equilibrate at 20º C and observed daily during the first week. The robotic screen produced three hits for the complex YU2 (core +V3): F105 Fab, that were optimized manually using hanging drop vapor-diffusion method. Diffraction quality crystals grew in droplets of 1µl of protein with 1 µl of reservoir solutions, which contained 16% PEG 6000, 200 mM ammonium sulfate, 8% 2-propanol, and 100 mM HEPES, pH 7.5

Deglycosylation, complex formation and crystallization of the gp120:b13 complex

The HXBc2 core gp120 variant containing 2-disulfide (W96C/V275C, I109C/Q428C)) and other stabilizing mutations (M95W, T257S/S375W, A433M) was constructed as previously described (*S6*). It was produced in free style 293F cells in the presence of 0.1 mM swainsonine and 10 µM kifunensine. The cell culture supernatant was purified by 17b affinity column and gp120 was eluted with 100 mM Glycine/HCl, pH 3.0 and immediately neutralized to pH 7.4 with Tris buffer. The purified gp120 was treated with endoglycosidase H_f (New England Biolabs) and passed through immobilized concanavalin A (Con-A Sepharose, Sigma) to remove any gp120 proteins with uncleaved N-linked glycans. The deglycosylated gp120 was combined with b13 Fab (molar ratio of b13 to gp120=1.2:1) to form a complex and purified with size exclusion chromatography (Superdex S75, GE Health). Purified complexes were concentrated to ~10 mg/ml, flash frozen with liquid nitrogen and stored in aliquots at -80 °C.

Crystallization trials for the gp120:b13 complex were setup robotically using vapor-diffusion sitting drops by mixing 0.1μl of protein with an equal volume of precipitant solutions (HoneyBee). 576 Conditions from our laboratory customized Hampton Crystal Screen (Hampton Research), Precipitant Synergy Screen (Emerald BioSystems) and Wizard Screen (Emerald BioSystems), were initially used. Diffraction quality crystal was obtained with hand optimization in 8% PEG8000, 6.5% Isopropanol, 200 mM $(NH_4)_2SO_4$, 100 mM HEPES, pH 7.5 at 20 °C.

Expression and purification of full length gp120 variant proteins

The full length YU2 gp120 variant proteins containing I109C or Q428C or both mutations were expressed in free style 293F cells and purified with histidine-tag affinity column. Previous studies have shown that the disulfide bond forms between cysteine 109 and 428 (*S6*). However, it is possible that the disulfide bond may not form for a small percentage of the double mutant protein. We expected the gp120 portion with unpaired cysteines to bind to antibody F105, whereas the gp120 portion with the 109-428 disulfide bond not to bind F105 (Table S4). To remove the portion of gp120 with unpaired cysteines, the I109C/Q428C gp120 was passed repeatedly over an antibody F105 column prior to being used for binding analysis.

X-ray data collection, structure determination and refinement for the gp120:F105 complex

Crystals were transferred to a cryoprotectant solution containing 20% glycerol, 24% PEG 6000, 8% 2-propanol and 100 mM HEPES pH7.5, soaked in Paratone-N (Exxon), loop

mounted, and flash-cooled to 100K for data collection. Data were collected at ID22 beam-line (SER-CAT) at the Advanced Photon Source, and processed and reduced with HKL2000 (*S7*).

The crystal structure was solved by molecular replacement with AMoRe (*S8*) in the CCP4 Program Suite (*S9*). To locate the position of F105 Fab in the complex, cross-rotation and translation searches with 50 different Fab models were performed. Only one solution was found using PDB ID code:1BBJ with Patterson correlation coefficient of 36.4% using 8-4 Å data. To find a second solution, we used three Fabs with high sequence similarity to F105 Fab found from the NCBI database. A new search model was constructed by combining portions of the three Fabs: 1RHH for the F105 light chain (residues 1-211), 1DNO for the F105 heavy chain variable domain (residues 1-123), and 1NOX for the F105 heavy chain constant domain (residues 124-218). The second solution gave a Patterson correlation coefficient of 40.5%.

F105-gp120 complex crystals belonged to the rhombohedral space group R32 with cell dimensions a=412.4 Å, b=412.4 Å c=83.2 Å and contained two molecules in the asymmetric unit. The two-Fab solution was rigid-body refined, and further subjected to density modification and two-fold NCS averaging to reduce model bias. The refined solution produced excellent gp120 electron density, where deviation of the V1/V2 stem region from that found in the CD4 bound conformation was evident. The gp120 was manually built into the σ_A-weighted *2Fo-Fc* density map using the program O (*S10*). The initial density of the β20/21 region, however, was not clear, but quality of the map around the region improved at the later stage of multiple iterative rounds of refinement using CNS (*S11*), REFMAC (*S12*), COOT (*S13*), and manual rebuilding. The V3 region was

completely disordered and the final map did not show any reasonable densities to trace the entire region (Figure S1). X-ray data and refinement statistics are summarized in Table S3.

X-ray data collection, structure determination and refinement for the gp120:b13 complex

gp120:b13 crystals were transferred into a 2 μl drop of cryoprotectant solution containing 15 % PEG8000, 10 % Isopropanol, 200 mM $(NH_4)_2SO_4$, 100 mM HEPES, pH 7.5, 20 % glycerol and immediately covered with immersion oil (MVH oil, Hampton Research). The crystals were then flash frozen in liquid nitrogen with a cryo loop (Hampton Research) and mounted under cryo condition (100K) for data collection. X-ray data were collected at beam-line ID-22 (SER-CAT) at the Advanced Photon Source, Argonne National Laboratory, with 1.0000 Å radiation, processed and reduced with HKL2000 (*S7*). Two forms of crystals were identified even though they are morphologically identical. Crystals with space group C222 diffracted to 2.5 Å and the other form with space group $C222_1$ diffracted to 3.2 Å, which contained two complexes per asymmetric unit.

The gp120:b13 complex structure was solved by molecular replacement with the program Phaser (*S14*) in the CCP4 Program Suite (*S9*) using the C222 data set (15-4 Å data used). A panel of 8 Fabs with varying elbow angles was used as initial searching models. Among all the searching models, Fab 1BBJ gave highest Z-scores (RFZ=6.6, TFZ=20.9). To thread the b13 sequences into the newly found search model, protein blast searches were performed with the sequences of b13 heavy and light chains, two Fab structures (1HEZ chain B and 1B6D chain A) in the Protein Data Bank gave high sequence similarities to the b13 heavy and light chains, respectively. The variable regions of 1HEZ:B (residues 1-128),

1B6D:A (residues 1-109) and b12's constant regions in 2NY7 (residues 129-230 for heavy chain and residues 110-211 for light chain) were separately superposed with the corresponding regions in 1BBJ. A new model was constructed by combining portions of the three Fabs: 1HEZ chain B for the variable region of b13 heavy chain, 1B6D for the variable region of b13 light chain, and 2NY7 for the constant domains of b13. To reduce model bias, the long CDR H3 was removed from the new model. With the new "hybrid" Fab model fixed, gp120 outer domain (residues 254-476) with β20/β21 regions trimmed was added to the searching process which yielded a high Z-score peak (RFZ=4.5, TFZ=24.4). The model with b13 Fab and the trimmed gp120 outer domain was subjected to several rounds of rigid body refinements from 6 Å to 3 Å using Refmac5 (*S12*). Further refinement was carried out with PHENIX (*S15*). Starting with torsion-angle simulated annealing with slow cooling, iterative manual model building was carried out on Xtalview (*S16*) and COOT (*S13*) with maps generated from combinations of standard positional, individual *B*-factor and TLS refinement algorithms. Ordered solvents were added during each macro cycle. The refined model of the C222 form was used as initial model for the $C222_1$ data set. Since the $C222_1$ form has two molecules per asymmetric unit, non-crystallographic symmetry (NCS) restraints were used during the refinement. Throughout the refinement processes, an R_{free} test set consisting of 5% of the data was used. X-ray crystallographic data and refinement statistics are summarized in Table S3.

Surface plasmon resonance analysis

To assess the binding kinetics of different ligands to HIV gp120 variants, CD4 and gp120 reactive antibodies 17b, m6, b3, b6, b11, b12, m14, m18, F91, F105, 15e were

directly immobilized onto CM5 sensor chips to surface densities of ~250 response units (RU) with standard amine coupling (Biacore). A test sensogram was run first for each analyte at a fixed concentration to evaluate the amplitude of binding response. The concentrations for all analytes were then adjusted accordingly in subsequent kinetics analysis so that the responses were below 100 RU for accurate data fitting. Increasing concentrations of gp120 variants were passed over coupled sensor chips at 30 μl/min for 3 min, followed by a 5-min dissociation phase. The buffer in all experiments was 10 mM HEPES, pH 7.4, 150 mM NaCl, 3 mM EDTA, and 0.01% surfactant P-20. Sensorgrams were fitted globally with BiaEvaluation 4.1 using a 1:1 Langmuir model of binding. Detailed kinetics data of the gp120 and gp140 variants binding to CD4 and antibodies are shown in Tables S5, S5 and S7.

FACS-based assay of antibody binding to cells expressing JR-FL gp160 envelope glycoproteins

Transfection of JR-FL envelope glycoprotein and FACS staining were performed as previously described (*S17, 18*). Initially, 8 x 10^6 293T cells in DMEM, 10% FBS, 1% pen-strep were plated onto a 150-mm tissue culture dish. The cells were transfected the following day with pSVIII expressor plasmids encoding wild-type JR-FL (cleavage-competent) or cleavage-defective glycoproteins, along with co-transfection of pctat expressor, using Fugene6 (Roche) at a DNA/Fugene6 ratio of 1:3 and 5 μg per 1x 10^6 cells. Forty-eight hours following transfection, the cells were harvested and washed in FACS buffer (1x PBS, 5% FBS, 0.02% azide) and dispensed into 96-wells V-bottom plates at 6 x 10^5 cells/well. A panel of ligands including IgG of b12, F105, b13, CD4, F91, b6, m18, 15e, and Fab of b12, F105, b3, b11, m14 were added to the wells at 0 to 100 μg/ml and incubated

for one hour. For each ligand tested, duplicate wells were done. The cells were washed in FACS buffer and Fluorescein (FITC)-conjugated anti-human IgG or Fab fragment (Jackson ImmunoResearch) at 1:300 dilutions was added for 30 min and then washed extensively to remove unbound secondary antibodies. The stained cells were analyzed by FACS on a BD LSR Flow Cytometer (BD Biosciences).

Numbering ofamino acid residues in antibodies

Kabat (*S19*) nomenclature was used to define positional numbering in antibody structures.

Graphical representations

Graphical representations of crystallographic structures were made with Pymol (*S20*) or GRASP (*S21*). GRASP was also used in calculations of molecular surfaces and volumes.

SUPPLEMENTARY FIGURES AND TABLES

Figure S1

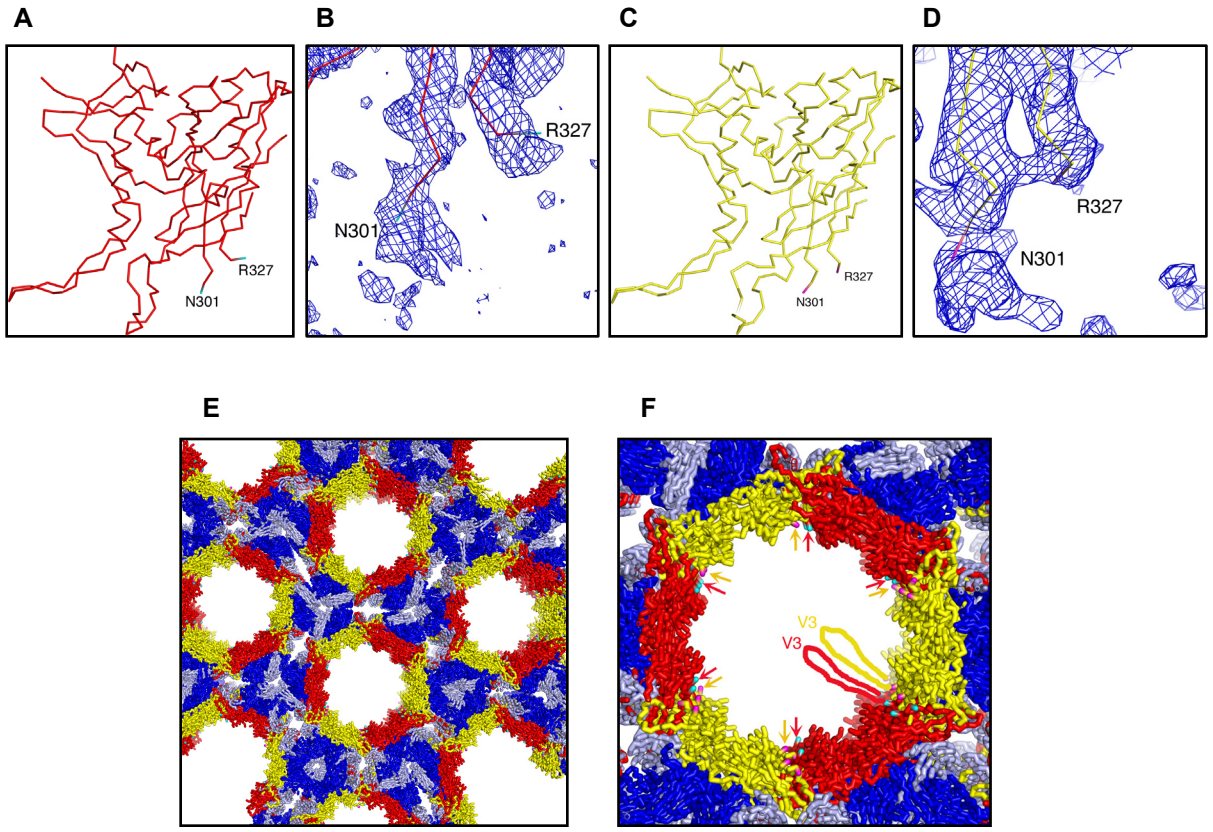

Figure S1. V3 region of F105-gp120 complex: structure, electron densities, and crystal packing

The V3 loop typically consists of 35 amino acids (range 31 to 39) and plays a number of important biological roles [reviewed in (*S22*)]. Not only is it critical for coreceptor binding (*S23*), but it also may interact with other elements in the viral spike to control the overall sensitivity of the virus to neutralization (*S24*). Previous structures of V3 (*S25, 26*) were obtained with gp120 in the CD4-bound state. Here we show the V3 loop, for gp120 bound to antibody F105. A: Cα tracing of the F105-bound gp120 conformation (molecule 1). N301 and R327, the starting and ending residues of the missing V3 loop, are labeled. B: Electron density (*2Fo-Fc* map at 1σ) around the V3 loop base of molecule 1. C: Cα tracing of the F105-bound gp120 conformation (molecule 2). D: Electron density (*2Fo-Fc* at 1σ) around the V3 loop base of molecule 2. E: Crystal packing of the complex in R32 space group; gp120 (red and yellow), F105 heavy chain (blue), F105 light chain (light blue). F: A close-up view of one of the hexagonal chambers in E. The arrows correspond to the V3 bases of two gp120s found in asymmetric units. Imaginary locations of untraceable segments (302-326) of the V3 loops are drawn in red and yellow.

Figure S2

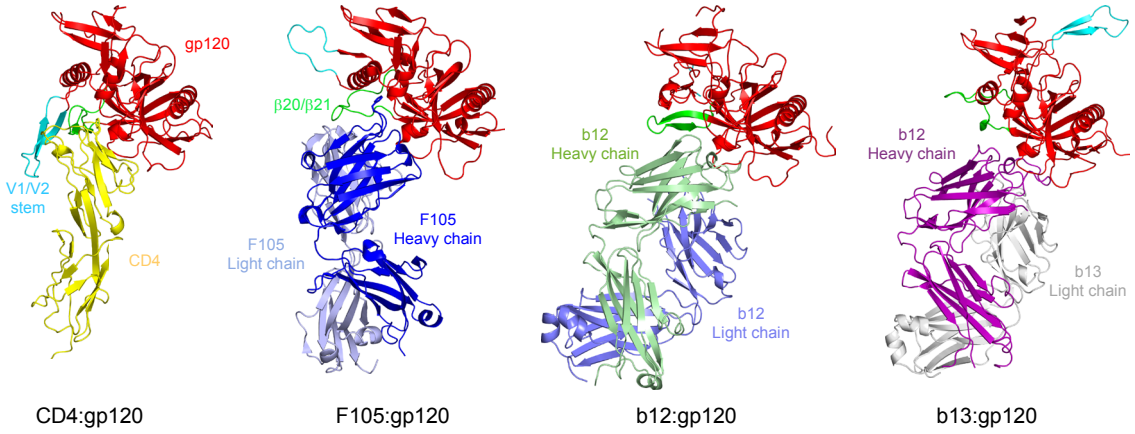

Figure S2. Angle of CD4, F105, b12, and b13 binding to gp120.
CD4-, F105-, b12-, and b13-Fab bound gp120 structures (red) are displayed with gp120s in the same orientation, as aligned by the structurally conserved outer domain. Although overall conformations of gp120 are similar, conformations of the V1/V2 stem (cyan) and b20-b21 strands (green) are unique. Interestingly, the angle of CD4 (yellow) binding to gp120 is similar to that of the F105 light chain (light blue). Also, b12 and b13 both use a heavy chain-only mode of binding and display similar angles of approach. It may be that the similarities in angles of approach observed here reflect structural constraints imposed by steric restrictions in the context of the oligomeric viral spike.

Figure S3

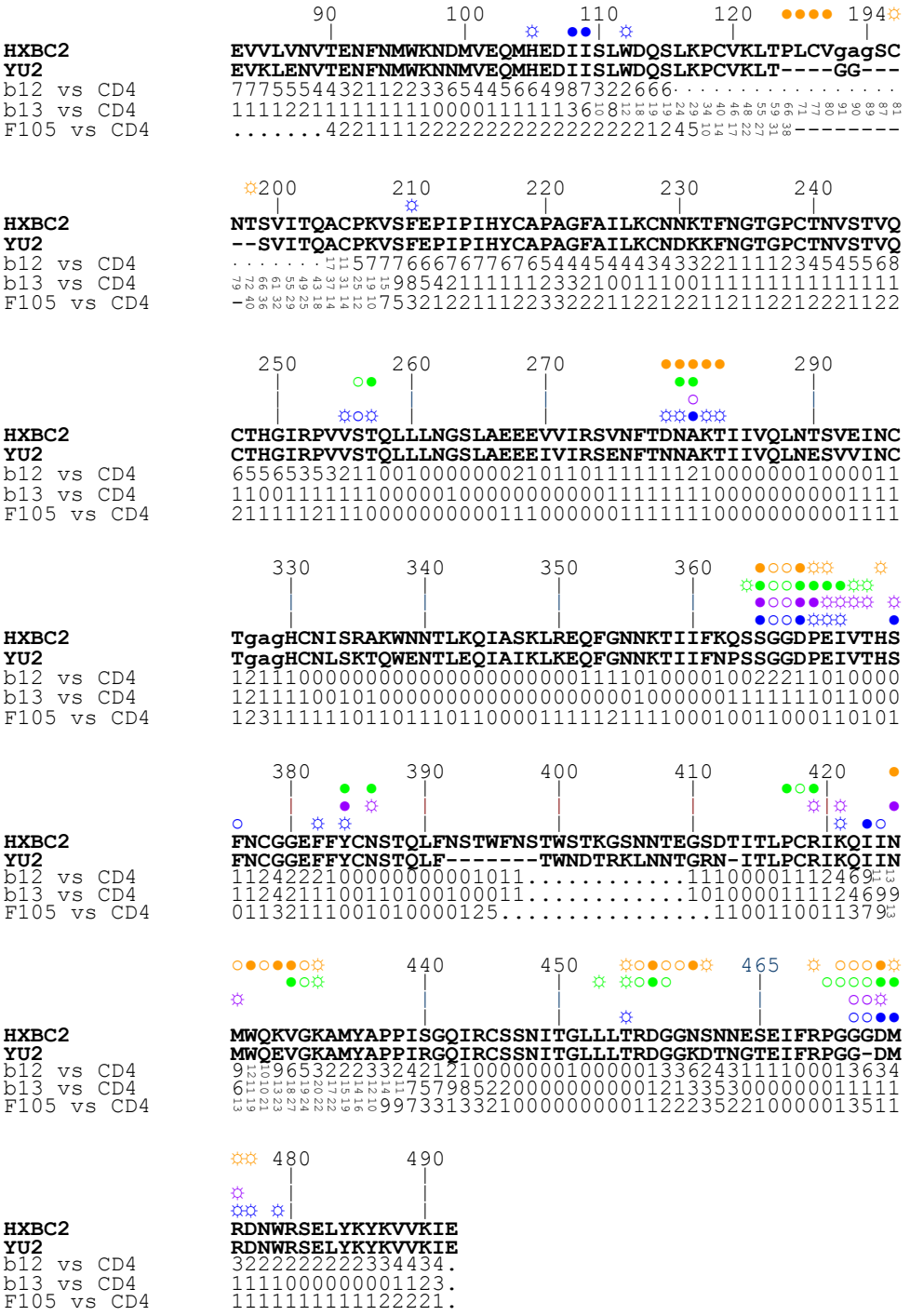

Figure S3. gp120 sequence, residue-by-residue contacts with CD4, b12, b13 and F105, and induced structural differences.

Both wild type HXBc2 core and YU2 core gp120 sequences are displayed with HxBc2 numbering convention, with the V1/V2 and V3 excursions replaced by Gly-Ala-Gly or Gly-Gly linkers. gp120 contacts as defined with the program MS (*S27*) for the b12, CD4, b13 and F105 complexes are indicated in orange, green, purple and blue symbols, respectively, with open circles denoting gp120 main-chain-only contacts, open circles with

rays denoting gp120 side-chain-only contacts, and filled circles denoting both main-chain and side-chain contacts. Structural difference between antibody- and CD4-bound states are shown with Cα distances (Å) between antibody- and CD4-bound structures of gp120 after outer domain superposition. Regions with no numbers are disordered and the "-" indicates there is no corresponding sequence for comparison. The V1/V2 and β20/β21 regions display remarkable variability in conformation among the different bound states.

Figure S4

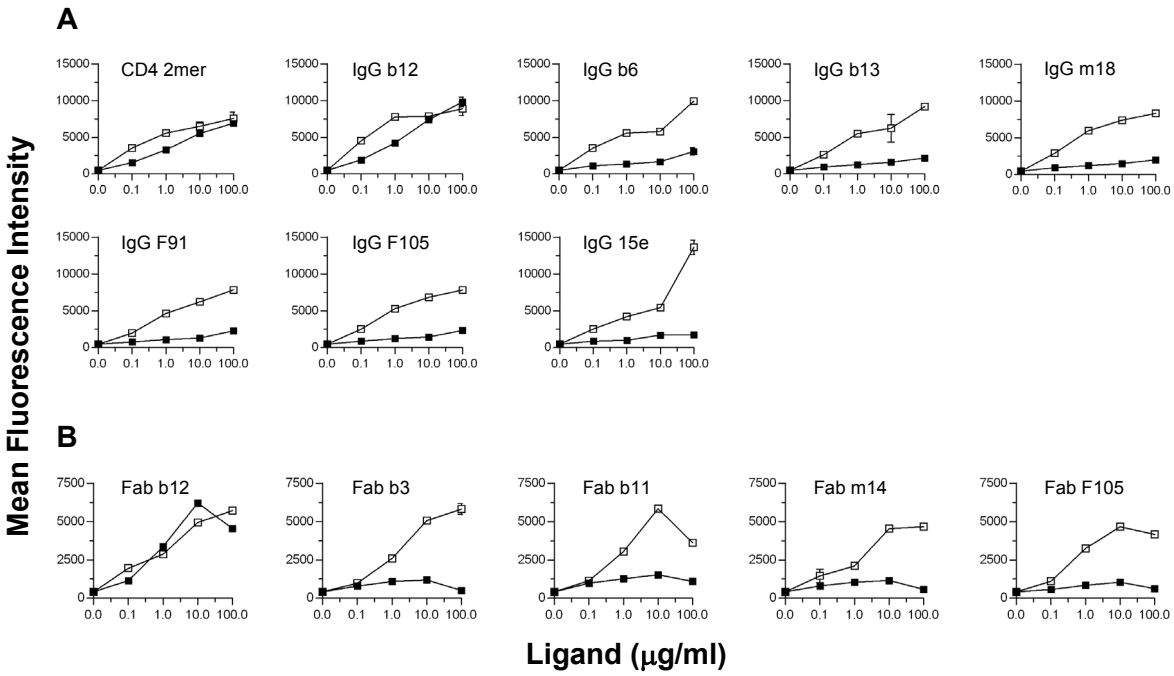

Figure S4. FACS-based cell-surface staining curves of JR-FL cleavage-competent and cleavage-defective envelope glycoproteins.

Cleavage between gp120 and gp41 is required for appropriate maturation of the HIV-1 viral spike, and this cleavage has significant effects on antigenic recognition. Thus antigenic recognition of cleaved cell-surface expressed JR-FL resembles neutralization sensitivity, with broadly neutralizing antibodies like b12 and 2G12 able to bind, but other antibodies like F105 and 17b, which can only neutralize laboratory-adapted isolates, unable to bind well. In contrast, antigenic recognition of uncleaved cell-surface expressed JR-FL does not resemble neutralization sensitivity, with antibodies like F105 and 17b able to bind as well as b12 and 2G12 (*S18*). Here we examine binding of the panel of CD4BS antibodies to cleaved and uncleaved cell-surface expressed JR-FL viral spikes. Cells (293T, transfected with plasmids encoding cleavage-competent (■) and cleavage-defective (□) JR-FL 160 glycoproteins) were stained and analyzed by FACS as described in Material and Methods with (**A**) CD4-IgG2 and CD4BS antibodies b12, b6, b13, m18, F105, F91,15e and (**B**) Fabs of CD4BS antibodies b12, b3, b11, m14, F105. For all of the ligands, the data shown are from a single representative experiment performed with duplicate samples. Error bars indicate the range of values obtained from the duplicates samples (for the more precise measurement, error bars are obscured by the size the symbols used to demark the results).

Table S1. Neutralization profiles of CD4, patient serum IgG and gp120-reactive antibodies against HIV-1 clade B and C reference viruses.

Tier/clade	Strain	CD4[#]			Patient 45 serum[§]	gp120-reactive antibodies														
						b12		b3	b6	b11	b13		m14	m18		F91	F105		15e	17b
		1mer	2mer	12mer	IgG	IgG	Fab	Fab	IgG	Fab	IgG	Fab	Fab	IgG	Fab	IgG	IgG	Fab	IgG	IgG
Tier 1/clade B	HXB2	0.045*	0.005	0.102	22	0.007	0.006	0.300	0.138	0.120	0.165	0.745	1.84	0.323	0.220	0.321	0.383	3.8	3.3	2.5
	MN.3	0.043	0.008	0.186	1.7	0.003	0.005	1.3	0.076	0.080	14.1	2.68	1.23	0.228	0.040	>50	>50	>50	>50	0.320
	SF162	1.7	0.526	2.1	11	0.062	0.093	24.3	8.7	3.3	15.7	16.2	42.9	19.5	5.3	>50	>50	>50	>50	21.0
	ADA	0.362	0.058	1.8	144	0.131	0.415	>50	7.4	15.9	37.5	24.8	>50	50.0	50.0	19.6	11.7	20.7	46.8	>50
	BaL.01	0.080	0.023	0.434	48	0.093	0.033	>50	>50	12.8	5.9	29.4	>50	>50	>50	>50	>50	>50	>50	>50
	BaL.26	0.140	0.044	0.709	49	0.051	0.021	23.5	17.3	2.7	4.2	10.8	35.6	22.3	13.5	22.9	16.8	23.8	>50	>50
	SS1196.1	0.640	0.460	1.8	33	0.680	1.1	44.6	9.3	12.3	7.7	8.2	18.8	15.7	5.5	10.4	15.3	9.64	29.4	5.9
Tier 2/clade B	JR-FL	2.5	0.525	0.048	74	0.030	0.046	>50	>50	>50	15.8	28	>50	>50	>50	>50	>50	>50	>50	>50
	YU2	0.480	0.100	0.510	208	1.8	6.9	>50	>50	>50	>50	>50	>50	>50	>50	>50	>50	>50	>50	>50
	89.6	0.580	0.166	2.5	132	0.140	0.659	>50	>50	>50	>50	>50	>50	>50	>50	>50	>50	>50	>50	>50
	6101.10	12.5	3.5	0.650	207	>50	48.0	>50	>50	>50	>50	>50	>50	>50	>50	>50	>50	>50	>50	>50
	7165.18	9.9	2.8	>50	340	>50	>50	>50	>50	>50	>50	>50	>50	>50	>50	>50	>50	>50	>50	>50
	6535.3	6.2	5.8	5.9	61	0.430	1.0	>50	50.0	10.7	>50	50.0	>50	>50	16.2	>50	50.0	>50	>50	>50
	QH0692.42	2.5	0.500	0.855	207	0.970	1.6	>50	>50	>50	>50	>50	>50	>50	>50	>50	>50	>50	>50	>50
	SC422661.8	11.0	5.2	1.6	107	0.440	0.454	>50	>50	>50	>50	>50	>50	>50	>50	>50	>50	>50	>50	>50
	PVO.4	8.7	24.2	6.0	195	>50	>50	>50	>50	>50	>50	>50	>50	>50	>50	>50	>50	>50	>50	>50
	TRO.11	>50	>50	28.8	208	>50	>50	>50	>50	>50	>50	>50	>50	>50	>50	>50	>50	>50	>50	>50
	AC10.0.29	>50	>50	1.1	207	1.8	3.0	>50	>50	>50	>50	>50	>50	>50	>50	>50	>50	>50	>50	>50
	RHPA4259.7	5.7	2.5	0.110	117	0.120	0.490	>50	>50	>50	>50	>50	>50	>50	>50	>50	>50	>50	>50	>50
	THRO4156.18	0.820	0.390	0.819	531	1.2	3.5	>50	>50	>50	>50	>50	>50	>50	>50	>50	>50	>50	>50	>50
	REJO4541.67	1.8	1.4	0.360	17	5.9	28.6	>50	>50	>50	>50	>50	>50	>50	>50	>50	>50	>50	>50	>50
	TRJO4551.58	39.3	>50	>50	163	>50	>50	>50	>50	>50	>50	>50	>50	>50	>50	>50	>50	>50	>50	>50
	WITO4160.33	14.8	2.2	0.262	312	8.5	4.9	>50	>50	>50	>50	>50	>50	>50	>50	>50	>50	>50	>50	>50
	CAAN5342.A2	28.0	49.8	1.0	388	>50	>50	>50	>50	>50	>50	>50	>50	>50	>50	>50	>50	>50	>50	>50
Tier 1/clade C	MW965.26	2.8	0.053	0.018	3.4	0.19	4.1	>50	>50	3.5	>50	>50	>50	>50	>50	>50	>50	>50	>50	0.250
Tier 2/clade C	Du151.2	6.8	1.4	0.052	248	24.4	>50	>50	>50	>50	>50	>50	>50	>50	>50	>50	>50	>50	>50	>50
	Du156.12	46.6	>50	0.389	115	0.750	3.8	>50	>50	>50	>50	>50	>50	>50	>50	>50	>50	>50	>50	>50
	Du172.17	1.6	0.293	0.072	349	0.300	1.9	>50	>50	>50	>50	>50	>50	>50	>50	>50	>50	>50	>50	>50
	Du422.1	19.1	26.9	0.493	>1000	0.464	2.3	>50	>50	>50	>50	>50	>50	>50	>50	>50	>50	>50	>50	>50
	ZM197M.PB7	7.6	16.7	50.0	605	>50	>50	>50	>50	>50	>50	>50	>50	>50	>50	>50	>50	>50	>50	>50
	ZM214M.PL15	29.7	>50	13.5	141	13.6	30.8	>50	>50	>50	>50	>50	>50	>50	>50	>50	>50	>50	>50	>50
	ZM233M.PB6	11.0	10.6	0.912	698	>50	>50	>50	>50	>50	>50	>50	>50	>50	>50	>50	>50	>50	>50	>50
	ZM249M.PL1	3.9	3.5	0.872	27	3.8	1.2	>50	>50	>50	>50	>50	>50	>50	>50	>50	>50	>50	>50	>50
	ZM53M.PB12	8.0	7.3	0.504	317	32.6	>50	>50	>50	>50	>50	>50	>50	>50	>50	>50	>50	>50	>50	>50
	ZM109F.PB4	0.200	0.066	0.034	62	>50	>50	>50	>50	>50	>50	>50	>50	>50	>50	>50	>50	>50	>50	>50
	ZM135M.PL10a	11.7	2.0	0.858	268	>50	>50	>50	>50	>50	>50	>50	>50	>50	>50	>50	>50	>50	>50	>50
	CAP45.2.00.G3	2.1	0.808	0.432	12	0.370	0.070	>50	>50	>50	>50	>50	>50	>50	>50	>50	>50	>50	>50	>50
	CAP210.2.00.E8	3.2	0.676	2.2	423	27.0	>50	>50	>50	>50	>50	>50	>50	>50	>50	>50	>50	>50	>50	>50
	CAP244.2.00.D3	8.4	3.5	2.5	256	>50	>50	>50	>50	>50	>50	>50	>50	>50	>50	>50	>50	>50	>50	>50	>50
Control	MuLV	>50	>50	>50	>1000	>50	>50	>50	>50	>50	>50	>50	>50	>50	>50	>50	>50	>50	>50	>50
Breadth[¥]		95%	87%	95%	97%	72%	67%	13%	18%	23%	21%	23%	13%	15%	18%	10%	13%	10%	8%	13%
Potency[¥]	Median	3.9	1.1	0.8	154	0.5	1.2	23.5	8.7	3.5	10.9	16.2	18.8	17.6	5.5	15.0	15.3	15.2	29.4	2.5
	Geometric mean	2.8	0.8	0.7	105	0.6	0.8	6.3	3.4	2.7	6.7	11.3	9.2	5.4	3.1	6.2	9.0	11.6	16.5	1.9

* Numerical values represent the concentrations (μg/ml) of CD4, patient serum IgG, or monoclonal antibodies (mAbs) required to achieve 50% neutralization (IC_{50}). Highlighted in red are IC_{50}s ≤ 1 μg/ml and in yellow are IC_{50}s between 1 and 50 μg/ml.

[#] Three forms of CD4 were tested: 1mer (monomer, N-terminal two domains of CD4 (*S28*)); 2mer (dimer, CD4 expressed in IgG2 format (*S29*)); 12mer (dodecamer, CD4 expressed in IgαTP format (*S30*)).

[§] Values are serum IgG concentrations required to achieve 50% neutralization (IC_{50}). Highlighted in purple are IC_{50} values of patient 45 serum IgG that was found to contain CD4BS directed neutralizing antibodies based on adsorption ratios of wild-type gp120 and a D368R mutant (details in Table S8).

[¥] For each antibody reagent, breadth was calculated as the percent of viral strains neutralized with an IC_{50} ≤ 50 μg/ml (mAbs) or ≤ 1000 μg/ml (serum IgG); Potency was calculated both as the median and geometric mean IC_{50} values for viral strains neutralized by ≤ 50 μg/ml mAbs or ≤ 1000 μg/ml serum IgG.

Table S2. Variational crystallization of CD4BS antibodies with HIV-1 gp120.

gp120	CD4BS antibody	Anti-V3 antibody	Crystallization Hits	Diffraction
YU2 core	15e		0	
	F91		0	
	F105		0	
	m14		0	
	m18		1	
YU2 (core +V3)	F105		3	2.9 Å
	F105	G3-299	1	none
	F105	G3-42	0	
JR-FL full length	F105		0	
	F105	G3-299	0	
	F105	G3-42	0	
			0	
HxBc2 core gp120*	b13		3	2.5/3.2 Å
	m18		1	none
YU2 Outer Domain	b13		1	none

* HxBc2 core gp120 with W96C, V275C, I109C, Q428C, M95W, T257S, S375W, 433M mutations
To enhance the opportunity of obtaining high quality crystal for diffraction experiments, different gp120 constructs were made to complex with a variety of CD4-binding site antibodies. Robotic crystallization screens were carried out with an initial trial of 576 conditions which were customized from commercially available kits (Hampton Crystal Screen of Hampton Research, Precipitant Synergy Screen and Wizard Screen of Emerald BioSystems). Crystal hits were then hand optimized to obtain higher quality crystals for data collection experiments.

Table S3. X-ray crystallographic data and model refinement statistics for gp120-F105 and gp120-b13 complexes

Data collection			
	gp120:F105	gp120:b13 Form 1[§]	gp120:b13 Form 2[§]
Space group	R32	C222	$C222_1$
Wavelength, (Å)	1.0000	1.0000	1.0000
Complexes per ASU	2	1	2
Unit cell constants (Å)			
a	412.4	112.6	106.2
b	412.4	204.0	204.3
c	83.2	109.3	216.9
α , β , γ (°)	90, 90, 120	90, 90, 90	90, 90, 90
Resolution (Å) *	50-2.9	50-2.5	50-3.2
Nominal resolution (Å) [#]	3.1	2.7	3.3
Completeness (%) *	75.5 (13.2)	78.1 (29.7)	86.5 (34.0)
No. of total reflections	209558	294025	187107
No. of unique reflections	48590	34810	35856
Redundancy *	4.4 (1.5)	8.5 (2.8)	5.2 (1.9)
R_{sym} (%) *	12.3 (51.5)	8.5 (43.4)	9.9 (45.0)
I/σ *	13.1 (1.2)	37.8 (1.5)	21.4 (1.7)
Refinement statistics ($\|F\| > 0\ \sigma$)			
Resolutions (Å)	43.5-2.9	39.2-2.5	43.2-3.2
No. of reflections	42563	34645	35358
R_{work} / R_{free} (%)	20.2 / 24.3	17.8 / 23.9	19.6 / 23.7
Average *B*-value (Å)	119.9	111.4	151.5
RMSD bond length (Å)	0.009	0.005	0.004
RMSD bond angles (°)	1.15	0.87	0.80
Ramachandran plot			
Favored (%)	91.3	93.1	88.2
Allowed (%)	99.0	99.9	98.1
PDB ID	3HI1	3IDX	3IDY

[§] These two forms of crystals appeared in the same growth condition. Average RMSD of Cα atoms between gp120 core, b13 heavy and light chains of the C222 and $C222_1$ forms are 0.6Å, 0.6Å and 0.4Å, respectively. RMSD of Cα atoms between corresponding molecules of the two complexes in the $C222_1$ form are 0.5Å, 0.3Å and 0.1Å for gp120 core, b13 heavy and light chains, respectively. CDR-H3 residues 100A-100C of Fab b13 in one complex of the $C222_1$ form assumes a slightly different conformation relative to that observed in the other asymmetric unit complex or in the C222 form.

* Values in parentheses are for the highest resolution shell. $R_{sym} = \Sigma \left| I - \langle I \rangle \right| / \Sigma \langle I \rangle$; I is the intensity of an individual measurement and <I> its mean value. $R_{work} = \Sigma |F_o - F_c| / \left| F_o \right|$; F_o and F_c are observed and calculated structure factors, respectively. R_{free}; same as *R* but calculated for a subset of the reflections (5%), which were omitted during the refinement and used to monitor its convergence.

[#] Resolution of a sphere with radius=1/(nominal resolution) that would be 100% complete when filled with measured reflections.

Table S4. Characterization by surface-plasmon resonance of the interaction between variants of HIV-1 Env and CD4, CD4-induced antibodies and CD4-binding-site antibodies.*

gp120	Ligands															
	CD4		CD4-induced antibodies				CD4-binding-site antibodies									
			17b		m6		b3	b6	b11	b12	b13	m14	m18	F91	F105	15e
	On ($\times 10^4$)	K_D (nM)	On ($\times 10^4$)	K_D (nM)	On ($\times 10^4$)	K_D (nM)	*K_D(Wild type)/K_D(Mutant)*									
Wild type	5.8	4.2	5.46	1.3	26.8	1.9	1	1	1	1	1	1	1	1	1	1
I109C	1.3	68.1	0.04	156	0.07	76.9	1.21×10^{-2}	1.91×10^{-3}	0.15	0.49	0.36	2.50×10^{-4}	1.19×10^{-2}	9.85×10^{-2}	4.07×10^{-2}	4.40×10^{-2}
Q428C	1.1	195	0.04	72.1	0.08	467	0.52	6.45×10^{-2}	0.36	0.28	5.70×10^{-2}	4.44×10^{-2}	4.91×10^{-2}	0.17	0.21	8.56×10^{-2}
Ds109/428	1.0	15.4	0.76	10.3	1.31	22.7	$< 10^{-5}$	$< 10^{-5}$	$< 10^{-5}$	0.13	1.24×10^{-4}	$< 10^{-5}$	$< 10^{-5}$	$< 10^{-5}$	$< 10^{-5}$	$< 10^{-5}$
OD1	nd	nd	nd	nd	nd	nd	$< 10^{-5}$	$< 10^{-5}$	$< 10^{-5}$	0.25	1.73×10^{-3}	$< 10^{-5}$	$< 10^{-5}$	$< 10^{-5}$	$< 10^{-5}$	$< 10^{-5}$
	On (gp140)/On gp120															
YU2	0.23		8.35×10^{-2}		5.78×10^{-2}		5.63×10^{-2}	1.04×10^{-2}	5.28×10^{-3}	0.19	2.19×10^{-2}	1.27×10^{-3}	2.85×10^{-2}	5.67×10^{-2}	6.87×10^{-2}	7.41×10^{-3}
JRFL	0.17		5.66×10^{-2}		5.23×10^{-2}		6.94×10^{-2}	1.70×10^{-2}	9.83×10^{-4}	0.18	1.40×10^{-2}	1.38×10^{-3}	2.09×10^{-2}	6.05×10^{-2}	3.24×10^{-2}	6.49×10^{-3}

* "On" refers to the on-rate, and K_D to the dissociation constant. "nd" refers to results that could not be determined, either because the off-rate was too fast (CD4) or on-rate too low (CD4-induced antibodies). Additional kinetic data are shown in Tables S5 and S7.

Table S5. Binding kinetics of CD4, CD4-induced and CD4BS antibodies to variant gp120s.

Analyte	Ligand--CD4		
gp120	on-rate ($M^{-1}s^{-1}$)	off-rate (s^{-1})	K_D(M)
YU2 WT	$5.80\times10^{4}\pm1.14\times10^{2}$	$2.44\times10^{-4}\pm2.34\times10^{-6}$	$4.21\times10^{-9}\pm4.12\times10^{-11}$
JRFL WT	$4.33\times10^{4}\pm1.49\times10^{2}$	$2.54\times10^{-4}\pm7.95\times10^{-7}$	$5.87\times10^{-9}\pm2.73\times10^{-11}$
YU2 I109C	$1.34\times10^{4}\pm1.42\times10^{2}$	$9.13\times10^{-4}\pm1.58\times10^{-6}$	$6.81\times10^{-8}\pm7.32\times10^{-10}$
YU2 Q428C	$1.13\times10^{4}\pm1.82\times10^{2}$	$2.20\times10^{-3}\pm3.81\times10^{-6}$	$1.95\times10^{-7}\pm3.15\times10^{-9}$
YU2 Ds109-428	$9.95\times10^{3}\pm2.07\times10$	$1.53\times10^{-4}\pm3.45\times10^{-6}$	$1.54\times10^{-8}\pm3.48\times10^{-10}$
YU2 OD1		No binding detected	

Analyte	Ligand--17b		
gp120	on-rate ($M^{-1}s^{-1}$)	off-rate (s^{-1})	K_D(M)
YU2 WT	$5.46\times10^{4}\pm7.53\times10$	$6.89\times10^{-5}\pm2.48\times10^{-6}$	$1.26\times10^{-9}\pm4.55\times10^{-11}$
JRFL WT	$6.38\times10^{4}\pm9.30\times10$	$1.26\times10^{-4}\pm2.75\times10^{-6}$	$1.97\times10^{-9}\pm4.35\times10^{-11}$
YU2 I109C	$3.85\times10^{2}\pm7.52\times10$	$5.99\times10^{-5}\pm6.93\times10^{-6}$	$1.56\times10^{-7}\pm3.53\times10^{-8}$
YU2 Q428C	$4.02\times10^{2}\pm17.6\times10$	$2.90\times10^{-5}\pm4.61\times10^{-7}$	$7.21\times10^{-8}\pm8.00\times10^{-9}$
YU2 Ds109-428	$7.60\times10^{3}\pm0.89\times10$	$7.84\times10^{-5}\pm2.58\times10^{-6}$	$1.03\times10^{-8}\pm3.40\times10^{-10}$
YU2 OD1		No binding detected	

Analyte	Ligand--m6		
gp120	on-rate ($M^{-1}s^{-1}$)	off-rate (s^{-1})	K_D(M)
YU2 WT	$2.68\times10^{5}\pm9.38\times10^{2}$	$5.10\times10^{-4}\pm4.99\times10^{-6}$	$1.90\times10^{-9}\pm1.98\times10^{-11}$
JRFL WT	$2.37\times10^{5}\pm7.95\times10^{2}$	$5.63\times10^{-4}\pm4.98\times10^{-6}$	$2.38\times10^{-9}\pm2.25\times10^{-11}$
YU2 I109C	$6.58\times10^{2}\pm4.57\times10$	$5.06\times10^{-5}\pm3.88\times10^{-6}$	$7.69\times10^{-8}\pm7.96\times10^{-9}$
YU2 Q428C	$7.84\times10^{2}\pm5.99\times10$	$3.66\times10^{-4}\pm2.82\times10^{-5}$	$4.67\times10^{-7}\pm5.07\times10^{-8}$
YU2 Ds109-428	$1.31\times10^{4}\pm1.13\times10$	$2.97\times10^{-4}\pm2.19\times10^{-6}$	$2.27\times10^{-8}\pm1.68\times10^{-10}$
YU2 OD1		No binding detected	

Analyte	Ligand--b3		
gp120	on-rate ($M^{-1}s^{-1}$)	off-rate (s^{-1})	K_D(M)
YU2 WT	$1.33\times10^{5}\pm3.99\times10^{2}$	$6.34\times10^{-4}\pm5.33\times10^{-6}$	$4.77\times10^{-9}\pm4.26\times10^{-11}$
JRFL WT	$1.23\times10^{5}\pm5.46\times10^{2}$	$5.50\times10^{-4}\pm9.00\times10^{-6}$	$4.47\times10^{-9}\pm7.58\times10^{-11}$
YU2 I109C	$4.96\times10^{3}\pm1.08\times10^{2}$	$1.96\times10^{-3}\pm1.50\times10^{-5}$	$3.95\times10^{-8}\pm9.12\times10^{-9}$
YU2 Q428C	$2.25\times10^{4}\pm1.13\times10^{2}$	$2.07\times10^{-4}\pm2.52\times10^{-6}$	$9.20\times10^{-9}\pm1.21\times10^{-10}$
YU2 Ds109-428		No binding detected	
YU2 OD1		No binding detected	

Analyte	Ligand--b6		
gp120	on-rate ($M^{-1}s^{-1}$)	off-rate (s^{-1})	K_D(M)
YU2 WT	$1.39\times10^{5}\pm1.54\times10^{2}$	$1.53\times10^{-5}\pm5.80\times10^{-7}$	$1.10\times10^{-10}\pm4.17\times10^{-12}$
JRFL WT	$9.14\times10^{4}\pm4.00\times10^{2}$	$3.13\times10^{-5}\pm5.89\times10^{-}$	$3.42\times10^{-10}\pm6.62\times10^{-12}$
YU2 I109C	$1.01\times10^{4}\pm6.48\times10$	$5.82\times10^{-4}\pm5.46\times10^{-6}$	$5.76\times10^{-8}\pm6.55\times10^{-10}$
YU2 Q428C	$5.80\times10^{4}\pm1.12\times10^{2}$	$9.90\times10^{-5}\pm4.48\times10^{-6}$	$1.71\times10^{-9}\pm7.73\times10^{-11}$
YU2 Ds109-428		No binding detected	
YU2 OD1		No binding detected	

Analyte	Ligand--b11		
gp120	on-rate ($M^{-1}s^{-1}$)	off-rate (s^{-1})	K_D(M)
YU2 WT	$1.02\times10^{4}\pm1.07\times10^{2}$	$2.17\times10^{-4}\pm9.12\times10^{-}$	$2.13\times10^{-8}\pm9.92\times10^{-10}$
JRFL WT	$1.80\times10^{4}\pm2.25\times10^{2}$	$9.25\times10^{-5}\pm1.53\times10^{-7}$	$5.14\times10^{-9}\pm6.48\times10^{-11}$
YU2 I109C	$1.34\times10^{4}\pm1.18\times10^{2}$	$1.85\times10^{-3}\pm9.46\times10^{-5}$	$1.38\times10^{-7}\pm7.16\times10^{-9}$
YU2 Q428C	$7.31\times10^{3}\pm1.88\times10^{2}$	$4.33\times10^{-4}\pm1.73\times10^{-5}$	$5.92\times10^{-8}\pm2.81\times10^{-9}$
YU2 Ds109-428		No binding detected	
YU2 OD1		No binding detected	

Analyte	Ligand--b12		
gp120	on-rate ($M^{-1}s^{-1}$)	off-rate (s^{-1})	K_D(M)
YU2 WT	$8.35\times10^{4}\pm1.58\times10^{2}$	$3.76\times10^{-3}\pm1.36\times10^{-5}$	$4.50\times10^{-8}\pm1.84\times10^{-10}$
JRFL WT	$7.06\times10^{4}\pm4.48\times10^{2}$	$4.74\times10^{-3}\pm1.89\times10^{-}$	$6.71\times10^{-8}\pm5.03\times10^{-10}$
YU2 I109C	$6.02\times10^{4}\pm1.06\times10^{2}$	$5.52\times10^{-3}\pm2.55\times10^{-5}$	$9.17\times10^{-8}\pm4.53\times10^{-10}$
YU2 Q428C	$2.73\times10^{4}\pm1.77\times10^{2}$	$4.38\times10^{-3}\pm1.27\times10^{-5}$	$1.60\times10^{-7}\pm1.14\times10^{-9}$
YU2 Ds109-428	$4.51\times10^{3}\pm2.95\times10$	$1.51\times10^{-3}\pm1.05\times10^{-5}$	$3.35\times10^{-7}\pm3.20\times10^{-9}$
YU2 OD1	$1.47\times10^{5}\pm1.07\times10$	$2.62\times10^{-2}\pm1.97\times10^{-4}$	$1.78\times10^{-7}\pm1.34\times10^{-9}$

Analyte	Ligand--b13		
gp120	on-rate ($M^{-1}s^{-1}$)	off-rate (s^{-1})	K_D(M)
YU2 WT	$2.22\times10^{4}\pm1.79\times10^{2}$	$3.23\times10^{-5}\pm2.39\times10^{-6}$	$1.45\times10^{-9}\pm1.08\times10^{-10}$
JRFL WT	$2.94\times10^{4}\pm1.32\times10^{2}$	$1.41\times10^{-4}\pm8.16\times10^{-6}$	$4.80\times10^{-9}\pm2.78\times10^{-10}$
YU2 I109C	$1.21\times10^{4}\pm1.10\times10^{2}$	$4.89\times10^{-5}\pm5.58\times10^{-6}$	$4.04\times10^{-9}\pm4.63\times10^{-10}$
YU2 Q428C	$8.07\times10^{3}\pm1.48\times10^{2}$	$2.06\times10^{-4}\pm7.08\times10^{-6}$	$2.55\times10^{-8}\pm9.94\times10^{-10}$
YU2 Ds109-428	$1.94\times10^{2}\pm3.02\times10$	$2.27\times10^{-3}\pm3.77\times10^{-5}$	$1.17\times10^{-5}\pm1.83\times10^{-6}$
YU2 OD1	$1.51\times10^{4}\pm1.59\times10^{2}$	$1.27\times10^{-2}\pm5.83\times10^{-5}$	$8.41\times10^{-7}\pm9.66\times10^{-9}$

Analyte	Ligand--m14		
gp120	on-rate ($M^{-1}s^{-1}$)	off-rate (s^{-1})	K_D(M)
YU2 WT	$4.26\times10^{4}\pm7.53\times10$	$1.76\times10^{-5}\pm1.73\times10^{-6}$	$4.13\times10^{-10}\pm4.06\times10^{-11}$
JRFL WT	$3.77\times10^{4}\pm2.23\times10^{2}$	$7.83\times10^{-5}\pm1.18\times10^{-7}$	$2.08\times10^{-9}\pm1.27\times10^{-11}$
YU2 I109C	$1.09\times10^{3}\pm1.33\times10^{2}$	$1.80\times10^{-3}\pm1.84\times10^{-5}$	$1.65\times10^{-6}\pm2.02\times10^{-7}$
YU2 Q428C	$2.85\times10^{4}\pm1.87\times10^{2}$	$2.65\times10^{-4}\pm4.40\times10^{-6}$	$9.30\times10^{-9}\pm1.66\times10^{-10}$
YU2 Ds109-428		No binding detected	
YU2 OD1		No binding detected	

Analyte	Ligand--m18		
gp120	on-rate ($M^{-1}s^{-1}$)	off-rate (s^{-1})	K_D(M)
YU2 WT	$2.28\times10^{5}\pm1.25\times10^{3}$	$2.43\times10^{-4}\pm2.66\times10^{-6}$	$1.07\times10^{-9}\pm1.30\times10^{-11}$
JRFL WT	$2.01\times10^{5}\pm9.16\times10^{2}$	$2.38\times10^{-4}\pm9.06\times10^{-6}$	$1.18\times10^{-9}\pm4.54\times10^{-11}$
YU2 I109C	$1.68\times10^{4}\pm1.71\times10^{2}$	$1.51\times10^{-3}\pm1.43\times10^{-5}$	$8.99\times10^{-8}\pm1.25\times10^{-9}$
YU2 Q428C	$2.65\times10^{4}\pm1.20\times10^{2}$	$5.75\times10^{-4}\pm4.79\times10^{-6}$	$2.17\times10^{-8}\pm2.06\times10^{-10}$
YU2 Ds109-428		No binding detected	
YU2 OD1		No binding detected	

Analyte gp120	Ligand--F91		
	on-rate ($M^{-1}s^{-1}$)	off-rate (s^{-1})	K_D(M)
YU2 WT	$1.44\times10^{5}\pm2.23\times10^{2}$	$1.85\times10^{-4}\pm5.90\times10^{-6}$	$1.28\times10^{-9}\pm4.10\times10^{-11}$
JRFL WT	$1.51\times10^{5}\pm5.84\times10^{2}$	$1.54\times10^{-4}\pm7.61\times10^{-6}$	$1.02\times10^{-9}\pm5.06\times10^{-11}$
YU2 I109C	$3.06\times10^{3}\pm7.77\times10$	$3.99\times10^{-5}\pm9.85\times10^{-6}$	$1.30\times10^{-8}\pm3.24\times10^{-9}$
YU2 Q428C	$3.19\times10^{4}\pm1.53\times10^{2}$	$2.43\times10^{-4}\pm3.59\times10^{-6}$	$7.62\times10^{-9}\pm1.18\times10^{-10}$
YU2 Ds109-428		No binding detected	
YU2 OD1		No binding detected	

Analyte gp120	Ligand--F105		
	on-rate ($M^{-1}s^{-1}$)	off-rate (s^{-1})	K_D(M)
YU2 WT	$7.60\times10^{4}\pm3.04\times10^{2}$	$8.48\times10^{-4}\pm9.57\times10^{-6}$	$1.12\times10^{-8}\pm1.34\times10^{-10}$
JRFL WT	$7.51\times10^{4}\pm3.22\times10^{2}$	$1.04\times10^{-3}\pm1.09\times10^{-5}$	$1.38\times10^{-8}\pm1.57\times10^{-10}$
YU2 I109C	$6.49\times10^{3}\pm1.89\times10^{2}$	$1.78\times10^{-3}\pm8.48\times10^{-6}$	$2.74\times10^{-7}\pm8.09\times10^{-9}$
YU2 Q428C	$2.28\times10^{4}\pm9.67\times10$	$1.19\times10^{-3}\pm3.94\times10^{-6}$	$5.22\times10^{-8}\pm2.81\times10^{-10}$
YU2 Ds109-428		No binding detected	
YU2 OD1		No binding detected	

Analyte gp120	Ligand--15e		
	on-rate ($M^{-1}s^{-1}$)	off-rate (s^{-1})	K_D(M)
YU2 WT	$1.93\times10^{4}\pm1.22\times10^{2}$	$1.47\times10^{-4}\pm5.76\times10^{-6}$	$7.62\times10^{-9}\pm3.02\times10^{-10}$
JRFL WT	$3.43\times10^{4}\pm8.52\times10$	$8.73\times10^{-5}\pm4.99\times10^{-6}$	$2.55\times10^{-9}\pm1.46\times10^{-10}$
YU2 I109C	$6.65\times10^{3}\pm2.21\times10^{2}$	$1.15\times10^{-3}\pm1.95\times10^{-5}$	$1.73\times10^{-7}\pm6.45\times10^{-9}$
YU2 Q428C	$7.54\times10^{3}\pm1.18\times10^{2}$	$6.71\times10^{-4}\pm1.01\times10^{-5}$	$8.90\times10^{-8}\pm1.93\times10^{-9}$
YU2 Ds109-428		No binding detected	
YU2 OD1		No binding detected	

Table S6. Rotation angles between different gp120-bound ligands

	b12	b13	F105	CD4
b12		16.7	53.4	110.0
b13			56.3	100.4
F105				139.7
CD4				

To quantify how the ligands approaching gp120, the complexes were superposed along the invariant gp120 outer domains, and then the approaching angles to gp120 for different ligands are compared. To calculate the rotation angles between different gp120-bound ligands, the gp120 complexes structures were first aligned against gp120 outer domain in the gp120-b12 complex. The pair wise rotation angles between different gp120-bound antibodies were then calculated by superposing their framework regions of both heavy and light chain variable domains in the gp120-outer-domain-aligned complexes. For comparison with CD4, only variable domain of heavy chain was used and the alignment was carried out as previously described (*S28*). Similarity between the approaching angles of b12 and b13 is evident; binding of F105 is in slightly different orientation which rotates about 50 degree away from that of b12. All superposition were performed with CCP4 package (*S9*).

Table S7. Association rates of CD4, CD4-induced and CD4BS antibodies to trimeric gp140 proteins

Ligands	gp140 foldon trimer	
	YU2	JR-FL
	on-rate ($M^{-1}s^{-1}$)	on-rate ($M^{-1}s^{-1}$)
CD4	$1.35\times10^{4}\pm4.00\times10$	$7.29\times10^{3}\pm4.32\times10$
17b	$4.56\times10^{3}\pm4.01\times10$	$3.61\times10^{3}\pm3.44\times10$
m6	$1.55\times10^{4}\pm4.82\times10$	$1.24\times10^{4}\pm3.70\times10$
b3	$7.49\times10^{3}\pm4.33\times10$	$8.54\times10^{3}\pm4.39\times10$
b6	$1.45\times10^{3}\pm7.82\times10$	$1.55\times10^{3}\pm1.50\times10$
b11	$5.39\times10\pm3.03$	$1.77\times10\pm2.77$
b12	$1.58\times10^{4}\pm1.10\times10^{2}$	$1.28\times10^{4}\pm2.44\times10$
b13	$4.87\times10^{2}\pm3.54\times10$	$4.21\times10^{2}\pm2.92\times10$
m14	$5.41\times10\pm7.89$	$5.20\times10\pm3.72$
m18	$6.50\times10^{3}\pm9.63\times10$	$4.20\times10^{3}\pm8.31\times10$
F91	$8.16\times10^{3}\pm4.49\times10$	$2.43\times10^{3}\pm3.58\times10$
F105	$5.22\times10^{3}\pm4.01\times10$	$3.61\times10^{3}\pm3.44\times10$
15e	$1.43\times10^{2}\pm7.50$	$2.33\times10^{2}\pm1.03\times10$

Table S8. Neutralization of HIV-1 clade B and C reference viruses by purified and pre-adsorped patient 45 serum IgG*.

Tier/clade	Strains	IC_{50} (µg/ml) after adsorption with				Percent neutralization[¥] based on IC_{50}s			IC_{80} (µg/ml) after adsorption with				Percent neutralization[¥] based on IC_{80}s		
		Blank	WT gp120	D368R gp120	WT/D368R IC_{50} ratio	gp120 directed	D368R gp120 directed	CD4BS directed	Blank	WT gp120	D368R gp120	WT/D368R IC_{80} ratio	gp120 directed	D368R gp120 directed	CD4BS directed
Tier 1/clade B	HXB2	9	288[§]	76	3.8	97%	88%	9%	47	500[§]	225	2.2	91%	79%	13%
	MN.3	2	30	35	0.9[#]	93%	94%	0%	5	60	66	0.9[#]	93%	93%	0%
	SF162	11	79	67	1.2[#]	86%	84%	3%	56	357	186	1.9[#]	84%	70%	17%
	BaL.01	25	71	105	0.7	65%	76%	0%	151	533	332	1.6	72%	55%	24%
Tier 2/clade B	JR-FL	17	88	44	2.0	81%	61%	24%	68	358	133	2.7	81%	49%	40%
	YU2	69	443	180	2.5	84%	62%	27%	232	1000[§]	443	2.3	77%	48%	38%
	6101.10	77	541	119	4.5	86%	35%	59%	479	2000[§]	930	2.2	76%	48%	36%
	6535.3	21	111	113	1.0	81%	81%	0%	310	519	359	1.4	40%	14%	66%
	SC422661.8	29	516[§]	240	2.2	94%	88%	7%	596[§]	1000[§]	745[§]	1.3	40%	20%	50%
	PVO.4	53	684[§]	298	2.3	92%	82%	11%	1000[§]	1000[§]	1000[§]	1.0	0%	0%	0%
	TRO.11	78	419	263	1.6	81%	70%	14%	618	2000[§]	815	2.5	69%	24%	65%
	RHPA4259.7	17	50	59	0.8[#]	65%	71%	0%	101	462	250	1.8[#]	78%	60%	24%
	REJO4541.67	14	46	112	0.4	70%	88%	0%	294	484	355	1.4	39%	17%	56%
	TRJO4551.58	171	934	304	3.1	82%	44%	46%	497	2000[§]	658	3.0	75%	24%	67%
Tier 1/clade C	MW965.26	1	500[§]	10	50.0	100%	87%	13%	4	500[§]	32	15.6	99%	88%	11%
Tier 2/clade C	Du156.12	62	997[§]	266	3.7	94%	77%	18%	445	1000[§]	809[§]	1.2	56%	45%	19%
	ZM214M.PL15	42	58	286	0.2	28%	85%	0%	1426[§]	2000[§]	1547[§]	1.3	29%	9%	67%
	ZM249M.PL1	55	357	209	1.7	85%	74%	13%	589[§]	1000[§]	710[§]	1.4	41%	17%	59%
	ZM109F.PB4	73	1119[§]	448	2.5	93%	84%	10%	915	2000[§]	2000[§]	1.0	54%	54%	0%
	CAP45.2.00.G3	20	63	206	0.3	68%	90%	0%	349	1189[§]	733	1.6	71%	52%	26%
	CAP244.2.00.D3	238	568	656	0.9	58%	64%	0%	1592[§]	2000[§]	2000[§]	1.0	20%	20%	0%

[*] Purified patient 45 serum IgG was pre-adsorped with blank, YU2 wild-type (WT) gp120 or D368R mutant beads to remove specific populations of gp120-reactive antibodies. Since the D368R mutation knocks out the binding of CD4BS-targeting antibodies (*S31*), the resultant IgG after D368R gp120 adsorption contained only CD4BS-targeting antibodies, as well as other non-gp120 reactive antibodies, while adsorption with WT gp120 removed all gp120-reactive IgG. Comparison of the HIV-1 neutralization by these pre-adsorped IgGs approximate the content of CD4BS-targeting antibodies elicited in patient sera. IC_{50} and IC_{80} ratios between WT gp120- and D368R gp120-adsorped IgGs were calculated, and were highlighted in purple if ≥ 2.

[#] These viruses are highly sensitive to V3, CD4i and other antibody specificities in polyclonal serum, a major CD4BS antibody neutralization effect would not be expected.

[§] IC_{50}s or IC_{80}s that were out of the measurable range were extrapolated from the fitted curve, or given a value of 500, 1000, or 2000 which was twice the highest concentration tested.

[¥] Percent neutralization is calculated as reduction in total neutralization by WT gp120 or D368R gp120 adsorptions relative to that of blank beads. The CD4BS directed neutralization is defined as further reduction of neutralization by WT gp120 adsorption relative to that of D368R gp120 (*S32*). In cases where the D368R neutralization titer was higher than WT (D368R gp120 adsorped more neutralization than WT gp120), a value of 0% was assigned.

Table S9. Distances from glycans to the Fab-contact surfaces on gp120

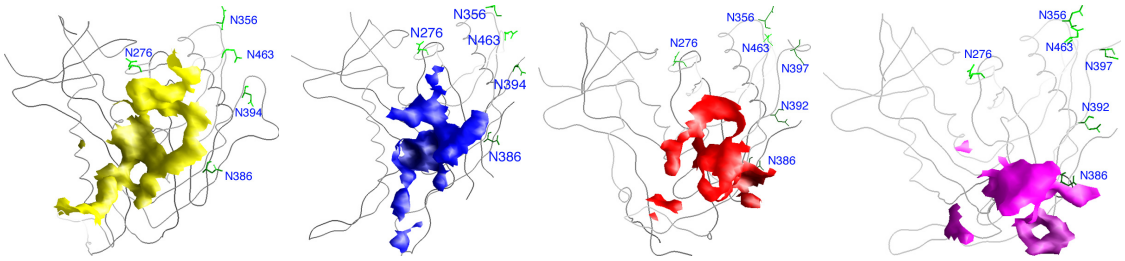

Distance (Å): Atom (Nδ2) center to Surface				
Nδ2	**CD4**	**F105**	**b12**	**b13**
234	16.2	16.7	19.0	20.0
241	28.4	28.4	28.5	31.1
262	16.0	11.9	14.9	16.3
276[#]	5.1	7.3	9.2	13.1
289	21.3	23.9	23.1	26.0
295	21.7	17.7	16.0	19.3
332	21.7	19.5	11.8	15.4
356	17.6	18.9	22.3	28.8
386	12.5	11.2	1.65	3.1
392[*]	--	--	10.7	11.5
394[*]	13.1	18.4	--	--
397[*]	--	--	18.1	23.7
413[*]	25.2	22.8	--	--
448	19.5	17.0	18.8	20.7
463	9.5	16.4	15.5	24.1

Distances from Nδ2 atoms of glycan-bearing ASN residues on gp120 to the contact surfaces on gp120 by CD4 (yellow), F105 (blue), b12 (red), and b13 (purple) are calculated using GRASP (*S21*).

[#] ASN residues that are located in vicinities of the epitopes are highlighted in blue.

[*] YU2 gp120, used for CD4 and F105-bound structures, shares the same glycosylation sites with the HXBc2 strain except that YU2 has glycosylated N394 and N413, whereas HXBc2 has glycosylated N392 and N397.

References

S1. Y. Li *et al.*, *Nat Med* **13**, 1032 (Sep, 2007).
S2. Y. Li *et al.*, *J Virol* **83**, 1045 (Jan, 2009).
S3. M. Li *et al.*, *J Virol* **79**, 10108 (Aug, 2005).
S4. M. R. Posner *et al.*, *J Immunol* **146**, 4325 (Jun 15, 1991).
S5. R. Wyatt *et al.*, *J Virol* **67**, 4557 (Aug, 1993).
S6. T. Zhou *et al.*, *Nature* **445**, 732 (Feb 15, 2007).
S7. Z. Otwinowski, W. Minor, *Methods Enzymol* **276**, 307 (1997).
S8. J. Navaza, *Acta Crystallographica Section A* **50**, 157 (1994).
S9. Collaborative Computational Project Number 4, *Acta Crystallographica Section D* **50**, 760 (1994).
S10. T. A. Jones, J. Y. Zou, S. W. Cowan, M. Kjeldgaard, *Acta Crystallogr A* **47 (Pt 2)**, 110 (Mar 1, 1991).
S11. A. T. Brunger *et al.*, *Acta Crystallogr D Biol Crystallogr* **54**, 905 (Sep 1, 1998).
S12. M. D. Winn, G. N. Murshudov, M. Z. Papiz, *Methods in Enzymology* **374**, 300 (2003).
S13. P. Emsley, K. Cowtan, *Acta Crystallographica Section D-Biological Crystallography* **60**, 2126 (2004).
S14. A. J. McCoy *et al.*, *Journal of Applied Crystallography* **40**, 658 (2007).
S15. P. D. Adams *et al.*, *Acta Crystallographica Section D* **58**, 1948 (2002).
S16. D. E. McRee, *J Struct Biol* **125**, 156 (Apr-May, 1999).
S17. M. Koch *et al.*, *Virology* **313**, 387 (Sep 1, 2003).
S18. M. Pancera, R. Wyatt, *Virology* **332**, 145 (Feb 5, 2005).
S19. E. A. Kabat, T. T. Wu, H. M. Perry, K. S. Gottesman, C. Foeller, *Sequences of Proteins of Immunological Interest.* (U.S. Department of Health and Human Services, National Institutes of Health, Bethesda, MD, ed. 5, 1991).
S20. W. L. DeLano, *The PyMOL Molecular Graphics System,* DeLano Scientific, San Carlos, CA, USA. http://www.pymol.org, (2002).
S21. A. Nicholls, K. A. Sharp, B. Honig, *Proteins* **11**, 281 (1991).
S22. O. Hartley, P. J. Klasse, Q. J. Sattentau, J. P. Moore, *AIDS Res Hum Retroviruses* **21**, 171 (Feb, 2005).
S23. S. S. Hwang, T. J. Boyle, H. K. Lyerly, B. R. Cullen, *Science* **253**, 71 (Jul 5, 1991).
S24. N. Sullivan *et al.*, *J Virol* **72**, 6332 (Aug, 1998).
S25. C. C. Huang *et al.*, *Science* **310**, 1025 (Nov 11, 2005).
S26. C. C. Huang *et al.*, *Science* **317**, 1930 (Sep, 2007).
S27. M. L. Connolly, *J Mol Graph* **11**, 139 (Jun, 1993).
S28. S. E. Ryu, A. Truneh, R. W. Sweet, W. A. Hendrickson, *Structure* **2**, 59 (Jan 15, 1994).
S29. G. P. Allaway *et al.*, *AIDS Res Hum Retroviruses* **11**, 533 (May, 1995).
S30. J. Arthos *et al.*, *J Biol Chem* **277**, 11456 (Mar 29, 2002).
S31. M. Thali *et al.*, *J Virol* **65**, 6188 (Nov, 1991).
S32. J. M. Binley *et al.*, *J Virol* **82**, 11651 (Dec, 2008).